Proceedings of the 11th ICPMG 2026
11th International Conference on Physical Modelling in Geotechnics
8-12 June 2026, Zurich, Switzerland

Vertical stress variation induced by helical pile installation in very dense sand

C.F. Silva
School of Engineering of São Carlos of the University of São Paulo, São Carlos, Brazil, silva.cf@usp.br

J.F. Michette
School of Engineering of São Carlos of the University of São Paulo, São Carlos, Brazil, jussaramichette@alumni.usp.br

C.H.C. Tsuha
School of Engineering of São Carlos of the University of São Paulo, São Carlos, Brazil, chctsuha@sc.usp.br

ABSTRACT: Helical piles have emerged as an effective solution for supporting power generation turbines in offshore wind farms. This is primarily due to their high tensile resistance, provided by the anchor effect of the helices, as well as the minimal disturbance they cause to the marine environment during installation. Understanding soil behavior during helical pile installation is crucial, as the process significantly influences the piles tensile capacity through the disturbances generated in the surrounding soil. This study examines the variation of vertical stresses around two single-helix pile models installed in a large calibration chamber filled with very dense dry sand. The piles featured 42.2 mm diameter shafts with helix diameters of 127 and 170 mm, embedded to a depth of 1000 mm. Vertical stresses were monitored using stress transducers installed at depths of 500, 750, 1000, and 1250 mm, each located 300 mm radially from the pile's central axis—corresponding to 1.8*D* and 2.4*D* from the longitudinal axes of piles 2 and 1, respectively, where *D* is the pile helix diameter. Results showed a modest increase in vertical stress as the helix approached each sensor depth, following the passage of the helix, the stresses gradually return to levels similar to those recorded prior to installation. Additionally, increasing helix diameter from 127 to 170 mm had negligible effect on vertical stress at the measured horizontal distance from pile axis, with both pile configurations displaying similar magnitudes and depth-related trends.

1 INTRODUCTION

Helical piles are increasingly prominent in the global geotechnical industry and have long served as reliable foundations for self-supporting transmission towers in the electricity and telecommunications sectors. Their straightforward installation, in-situ control of load-bearing capacity, and resistance to both tensile and compressive forces have significantly broadened their range of applications. Features such as load capacity monitoring during installation via torque measurements, and the ability to be installed at an angle to resist horizontal loads, have extended their use beyond traditional contexts. Today, helical piles are employed in the foundations of decks, bridges, temporary structures, and both residential and commercial buildings. Additionally, among the various options for offshore wind farm foundations, helical piles have emerged as particularly attractive due to their high tensile capacity, which arises from the "anchor effect" of the helices (Spagnoli & Gavin, 2015; Al-Baghdadi et al., 2015; Fateh et al., 2017; Spagnoli et al., 2018). Their rapid installation and potential for reuse make helical pile foundations especially advantageous for offshore wind turbine applications (Ding et al., 2019).

The installation process plays a crucial role in determining the tensile capacity of piles used as foundations for transmission line towers and onshore or offshore wind turbines. This process influences the surrounding soil conditions through the penetration of the helices, which can affect the pile's performance under tensile loads and potentially reduce the foundation's overall load-bearing capacity. Accordingly, a thorough understanding of soil behaviour during installation is essential, as the disturbances introduced by the helices significantly impact the tensile capacity of the piles.

This study evaluates the variation in vertical stresses induced by the installation of two helical pile models with different helical plate diameters, installed in a large calibration chamber filled with very dense sand prepared under controlled density conditions.

2 EXPERIMENTAL PROGRAM

2.1 Materials, equipment and instrumentation

Numerous studies have conducted field tests on helical piles in a variety of soil types. However, these tests often lack control over the soil stress conditions, making accurate calibration of performance prediction models challenging. In contrast, physical modeling techniques, where pile tests are performed under controlled soil and confining stress conditions, have proven successful in investigating this type of foundation. Among these techniques, calibration chamber tests and geotechnical centrifuge tests are the most commonly employed, as they can effectively replicate field stress environments.

Calibration chamber studies are employed when precise control of boundary conditions is required. In this approach, a sample of known material and density is systematically prepared to fill the chamber, allowing tests to be conducted under controlled stress and deformation states. This methodology effectively minimises the influence of natural soil variability on test outcomes. Calibration chambers have been instrumental in establishing empirical correlations for estimating geotechnical parameters from in-situ soil investigation tests such as standard penetration test (SPT) and the cone penetration test (CPT), and are also widely used for calibrating in-situ testing equipment under controlled conditions.

In this investigation, experiments were carried out within a calibration chamber constructed at the Experimental Site of the University of São Paulo at São Carlos, Brazil (EESC/USP). This apparatus allowed the simulation of field stress conditions at the depth corresponding to the helical pile helices embedded in very dense dry sand (Dr = 97%). The calibration chamber comprises a steel tank, a top cover, a rubber membrane, an air-pluviation system, and reaction frames (Figures 1 and 2).

The cylindrical steel tank has an internal diameter of 1.2 m and a height of 1.5 m. During the tests, vertical surcharges of 50, 100, and 150 kPa were applied using a rubber membrane inflated with air and placed atop the sand bed. To minimise side friction between the sand and the tank walls, a latex rubber sheet coated externally with silicone grease was attached to the interior surface of the tank.

In this study, two distinct model piles were fabricated for installation and testing within dry sand specimens prepared using the air-pluviation method inside a calibration chamber. During all experiments, soil stress sensors were used to monitor vertical stress variations in the soil during pile installation. Six test series were conducted to evaluate the installaion of the two model piles under three levels of applied vertical surcharge (50, 100, and 150 kPa).

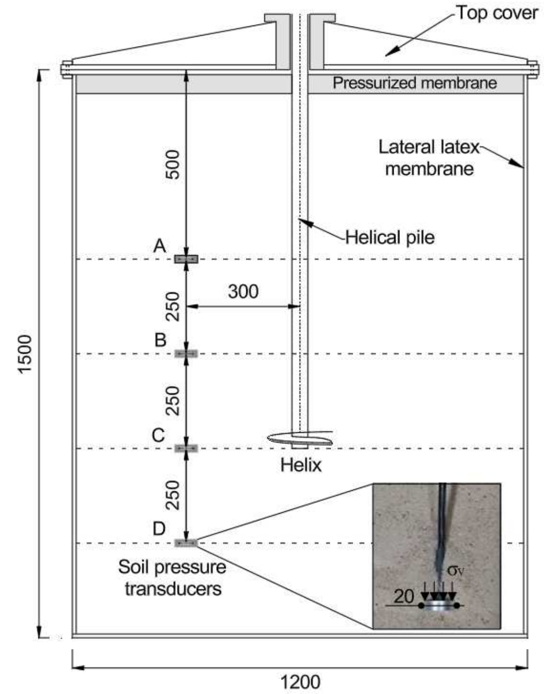

Figure 1. Schematic of the calibration chamber with pile model and pressure transducer details (dimensions in mm).

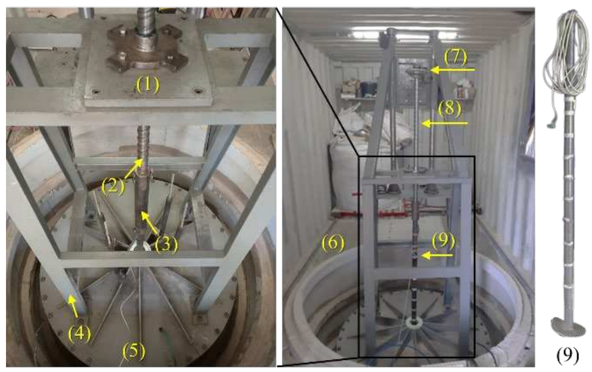

1 – Nut (centralizing device)
2 – Threaded rod
3 – Connection sleeve
4 – Instalation suport structure
5 – Top cover
6 – Instalation suport structure
7 – Chain gear
8 – Threaded rod
9 – Pile model

Figure 2. Helical pile installation system.

2.2 Sand bed

The air-pluviation method was used to prepare six dry sand samples within the chamber tank. The silica sand employed in this study had been previously characterised by Silva and Tsuha (2021). The material comprised angular to sub-angular grains with an average particle size (d_{50}) of 0.18 mm. Key properties of the sand used in the experiments are summarised in Table 1.

Table 1. Sand properties

Property	Value
Specific gravity of the sand particles, G_s	2.67
Maximum dry unit weight, $\gamma_{d(\max)}$	17.65 kN/m³
Minimum dry unit weight, $\gamma_{d(\min)}$	14.35 kN/m³
Average dry unit weight of sand samples, $\gamma_{d(avg)}^{*}$	17.56 kN/m³
Maximum void ratio, e_{max}	0.83
Minimum void ratio, e_{min}	0.48
Relative density of the sand sample, D_r	97%
Average grain size, d_{50}	0.18 mm
Coefficient of uniformity, C_u	1.73
Particle shape	Angular to sub-angular
Peak friction angle from direct shear tests, ϕ_{peak}	39.8º
Constant-volume friction angle from triaxial tests, ϕ_{cv}	31.0º

* Estimated by weighing samples placed in the tank (dividing the weight by the sample volume).

To determine the relative density of the sand, an independent test was conducted in which the chamber tank was filled using a carefully controlled air-pluviation process, without pile installation. Sand density was measured by collecting the mass of six calibrated density pots placed at different elevations within the central region of the sand bed during pluviation. The resulting dry unit weights (γ_d) ranged from 17.51 to 17.60 kN/m³, with an average of 17.56 kN/m³, corresponding to an average relative density (D_r) of 97%.

2.3 Soil measurements

Pressure transducers were used to measure vertical stresses within the soil mass. The sensors were installed at four depths (500, 750, 1000, and 1250 mm) and positioned 300 mm from the longitudinal axis of the pile during the pluviation process.

The location of the soil sensors is shown in Figure 1. Pluviation was paused upon reaching the designated installation level to allow careful placement of each transducer within the sand bed. The pressure transducers, with a measurement range of 0–500 kPa and dimensions of 20 mm in diameter and 7 mm in thickness, were manufactured by Geoinstrumentos (Brazil), which also provided the calibration constants determined via air pressurisation..

2.4 Model piles

Two model piles were fabricated with a close-ended steel tubular shaft of 42.2 mm external diameter (d) and 9 mm wall thickness, and a steel helical plate of 127 mm and 170 mm diameter (D), 6.4 mm thickness and 40 mm helix pitch. The dimensions of the piles are illustrated in Figure 3.

A total of six pile installations were carried out in this study, with each pile installed under three distinct confining stress conditions of 50, 100, and 150 kPa.

Due to the larger diameter of the model pile helix relative to the central opening of the top membrane, initial manual installation was required. The lower segment of each pile was inserted into the sand by applying torque to a depth of approximately 10 cm below the top cover. The upper membrane and top cover were then installed, as shown in Figure 1, and the membrane was subsequently inflated and pressurized using a controlled pressure system.

Pile installation was carried out through the central openings of the top cover and membrane using an electric motor mounted on a steel frame above the chamber, at a rotation rate of 12 revolutions per minute. Displacement control was employed to ensure vertical advancement of one helix pitch per revolution, following recommended practices to minimise soil disturbance and optimise pile performance (Perko, 2009; Lutenegger et al., 2015). Installation was stopped once the helix reached a depth of 1.0 m below the top cover.

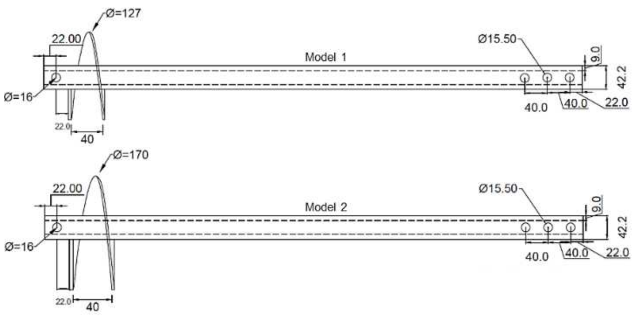

Figure 3. Helical pile models used in this study (dimensions in mm).

3 RESULTS AND DISCUSSION

The variation of the vertical stresses (σ_v) within the soil sample along its depth during pile installation is presented individually in Figures 4–6 and Tables 2–3, corresponding to confining stresses of 50, 100, and 150 kPa.

Tables 2–3 present the vertical stresses recorded by the pressure transducers positioned around the helix at the moment the pile reached the corresponding installation depths of 500, 750, and 1000 mm. For example, as illustrated in Figure 1, when the helix reaches a depth of 500 mm, it aligns with pressure transducer A, whose measured stress corresponds to $\sigma_{v,50}$ (the vertical stress at a depth of 500 mm). The same measurements were recorded by transducers B and C at depths of 750 mm and 1000 mm, respectively, and $\sigma_{v,75}$ and $\sigma_{v,100}$ were registered

For pressure transducer D, installed at a depth of 1250 mm, no direct measurements of stresses around the helix were obtained, as pile installation stopped at a depth of 1000 mm. Only the residual stresses propagated to the bottom of the chamber were recorded.

The vertical stresses at a depth of 0.0 m represent the stresses applied by the pressurized membrane at the top of the sand sample and were measured and regulated using a manometer connected to the pressure control system. Table 4 presents the vertical stresses recorded by the pressure transducers at the moment the helix reached their respective installation depths of 500, 750, and 1000 mm.

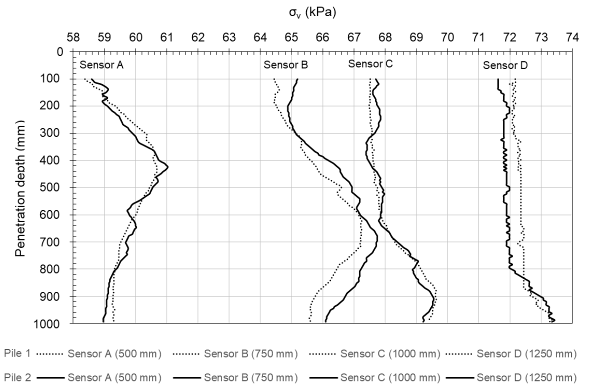

Figure 4. Variation of vertical stresses along the depth during the installation of piles 1 and 2, for an applied vertical surcharge of 50 kPa by the membrane.

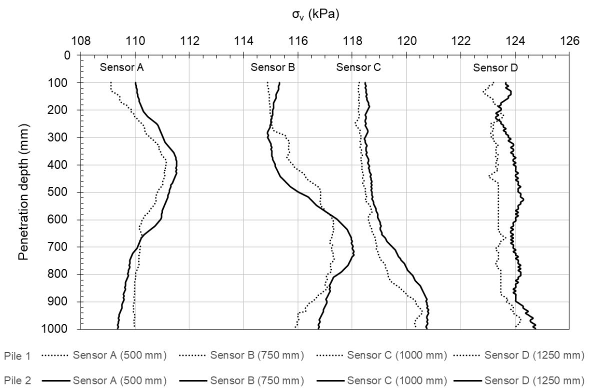

Figure 5. Variation of vertical stresses along the depth during the installation of piles 1 and 2, for an applied vertical surcharge of 100 kPa by the membrane.

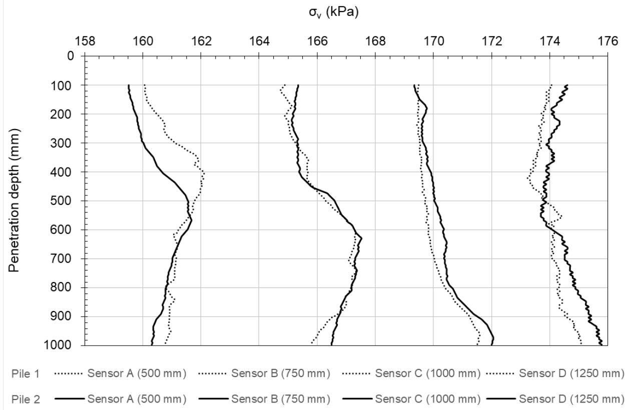

Figure 6. Variation of vertical stresses along the depth during the installation of piles 1 and 2, for an applied vertical surcharge of 150 kPa by the membrane.

Table 2. Vertical stresses recorded by the pressure transducers during the installation of model pile 1 (D = 127 mm).

Applied vertical surcharge (kPa)	Pressure transducer	Transducer depth (cm)	$\sigma_{v,avg}$ (kPa)	Coefficient of variation (%)	$\sigma_{v,max}$ (kPa)	$\sigma_{v,50}$ (kPa)	$\sigma_{v,75}$ (kPa)	$\sigma_{v,100}$ (kPa)
50	A	50	59.7	1.0	60.7	60.5	59.5	59.3
	B	75	65.9	1.4	67.2	66.6	66.9	65.6
	C	100	68.2	1.1	69.6	67.7	68.8	69.4
	D	125	72.4	0.4	73.3	72.3	72.4	73.3
100	A	50	110.3	0.5	111.2	110.8	110.1	110.0
	B	75	116.3	0.7	117.3	116.8	117.3	115.9
	C	100	118.9	0.6	120.6	118.5	119.1	120.3
	D	125	123.4	0.2	124.2	123.4	123.4	124.0
150	A	50	161.1	0.3	162.1	161.8	161.1	160.8
	B	75	166.2	0.5	167.3	166.3	167.3	165.8
	C	100	170.0	0.4	171.6	169.7	170.2	171.5
	D	125	174.1	0.3	175.2	173.8	174.3	175.2

$\sigma_{v,avg}$ = average vertical stress; $\sigma_{v,max}$ = maximum vertical stress; $\sigma_{v,i}$ = vertical stress measured at depth "i".

Table 3. Vertical stresses recorded by the pressure transducers during the installation of model pile 2 (D = 170 mm).

Applied vertical surcharge (kPa)	Pressure transducer	Transducer depth (cm)	$\sigma_{v,avg}$ (kPa)	Coefficient of variation (%)	$\sigma_{v,max}$ (kPa)	$\sigma_{v,50}$ (kPa)	$\sigma_{v,75}$ (kPa)	$\sigma_{v,100}$ (kPa)
50	A	50	59.7	1.0	61.0	60.5	59.7	59.0
	B	75	66.4	1.4	67.7	66.9	67.5	66.1
	C	100	68.2	1.0	69.6	67.9	68.8	69.2
	D	125	72.1	0.6	73.4	72.0	72.1	73.3
100	A	50	110.4	0.6	111.5	111.3	109.8	109.4
	B	75	116.4	1.0	118.1	116.0	117.9	116.7
	C	100	119.3	0.7	120.8	118.7	119.9	120.8
	D	125	124.0	0.2	124.8	124.1	124.1	124.8
150	A	50	160.6	0.4	161.7	161.6	160.9	160.3
	B	75	166.3	0.5	167.5	166.6	167.3	166.5
	C	100	170.3	0.4	172.1	170.0	170.5	172.0
	D	125	174.5	0.3	175.8	173.8	174.8	175.8

Table 4. Vertical stresses recorded during helix passage at the sensor depth during the installation of piles 1 and 2.

Depth (mm)	D (mm)	127 (pile 1)			170 (pile 2)		
0	$\sigma_{v,0}$ (kPa)	50.0	100.0	150.0	50.0	100.0	150.0
500	$\sigma_{v,50}$ (kPa)	60.5	110.8	161.8	60.5	111.3	161.6

750	$\sigma_{v,75}$ (kPa)	66.9	117.3	167.3	67.5	117.9	167.3
1000	$\sigma_{v,100}$ (kPa)	69.4	120.3	171.5	69.2	120.8	172.0

Figures 4–6 show a modest increase in vertical stress as the pile helix penetrates the soil at depths corresponding to the locations of the stress transducers. Once the helix passes, the measured stresses generally return to a residual value that remains stable and closely approximates the initial pre-installation conditions. This variation is most pronounced for transducers A and B, which capture deformations in the soil mass adjacent to the cylindrical zone disturbed by the helix. These deformations account for the observed fluctuations in vertical stress, with alternating increases and decreases as the helix advances.

In contrast, transducers C and D, located near the helix at depths of 1000 mm and 1250 mm, respectively, exhibited only increases in vertical stress as the helix advanced, without the oscillations observed at shallower depths. This pattern of vertical stress variation was consistent across all three applied vertical surcharge levels (50, 100, and 150 kPa) and was repeated along the entire installation path for both pile models.

The analysis of mean values and stress variations recorded by the transducers, presented in Tables 2 and 3, indicates that vertical stresses at depths of 500, 750, 1000, and 1250 mm, measured at a radial distance of 300 mm from the pile axis (~1.8D for pile 2 and 2.4D for pile 1), remained essentially unchanged during installation compared to resting conditions. In most cases, the coefficients of variation were below 1%, indicating a low degree of stress heterogeneity throughout the installation process. Furthermore, the results show that increasing the helix diameter from 127 mm to 170 mm had a negligible effect on the measured vertical stresses at these radial distances, with values remaining comparable and exhibiting similar patterns across all depths, as summarised in Table 4.

4 CONCLUSIONS

Understanding the variation of soil stresses during the installation of helical piles is essential for developing reliable design methods, as the disturbances caused by the helices significantly influence the tensile capacity of the piles. In this context, the present study investigates the variation of vertical stresses at radial distances of 1.8D and 2.4D from the pile axis (where D is the helix diameter) induced during the installation of two helical pile models in a very dense sand in a calibration chamber and subjected to vertical surcharge pressures of 50, 100, and 150 kPa.

At the evaluated distances (1.8D and 2.4D from the pile axis), a slight increase in vertical stress was observed as the helix reached the level of the stress transducers; however, the stresses generally returned to stable residual values comparable to pre-installation conditions.

Overall, the vertical stress distribution remained essentially unchanged throughout installation at the evaluated radial distances, irrespective of the applied vertical surcharge level.

ACKNOWLEDGEMENTS

The authors would like to acknowledge the financial support given by the National Council for Scientific and Technological Development – CNPQ for the financial support of this work (Process 142166/2019-7) and for granting the doctoral scholarship of the first author.

REFERENCES

Al-Baghdadi, T.A.; Brown, M.J.; Knappett, J.A.; Ishikura, R. (2015) Modelling of Laterally Loaded Screw Piles with Large Helical Plates in Sand. In: *Frontiers in Offshore Geotechnics III - Proceedings of the International Symposium on Frontiers in Offshore Geotechnics*. Taylor & Francis Group: London. p. 503 – 508.

Ding, H.; Wang, L.; Zhang, P.; Liang, Y.; Tian, Y.; Qi, X. (2019) The Recycling Torque of a Single-Plate Helical Pile for Offshore Wind Turbines in Dense Sand. *Applied Sciences*, 9(19).

Fateh, A.M.A.; Eslami, A.; Fahimifar, A. (2017) Direct CPT and CPTu Methods for Determining Bearing Capacity of Helical Piles. *Marine Georesources & Geotechnology*, 35(2): 193 – 207.

Lutenegger, A.J.; Tsuha, C.H.C. (2015) Evaluating Installation Disturbance from Helical Piles and Anchors Using Compression and Tension Tests. In: *Proceedings of the 15th Pan-American Conference on Soil Mechanics and Geotechnical Engineering*, Buenos Aires, p. 373 – 381.

Perko, H. A. (2009) *Helical Pile: A Practical Guide for Design and Installation*. Hoboken, New Jersey: John Wiley & Sons. p. 528.

Silva, D. M. and Tsuha, C.H.C. (2021) Experimental Investigation on the Installation and Loading Performance of Model-Scale Deep Helical Piles in Very Dense Sand. *Canadian Geotechnical Journal*, 58(9): 1379 – 1395.

Spagnoli, G.; Gavin, K. (2015) Helical Piles as a Novel Foundation System for Offshore Piled Facilities. In:

Proceedings of the Abu Dhabi International Petroleum Exhibition and Conference, Abu Dhabi, UAE, 2015.

Spagnoli, G.; Solarte, C.M.M.; Tsuha, C.H.C; Oreste, P. (2018) Parametric Analysis for the Estimation of the Installation Power for Large Helical Piles in Dry Cohesionless Soils. *International Journal of Geotechnical Engineering*, 14(5): 569 – 579.